Evidence for Transcranial Magnetic Stimulation Induced Functional Connectivity Oscillations in the Brain*

Victor M. Vergara, Farshad Rafiei, Martijn E. Wokke, Hakwan Lau, Dobromir Rahnev, and Vince D. Calhoun, *Member, IEEE*

Abstract— **Transcranial magnetic stimulation (TMS) is an effective research tool to elucidate mechanisms of function in the brain. Despite its widespread use, very few studies have looked at dynamic functional connectivity responses to TMS. This work performs an exploratory analysis of dynamic functional network connectivity (dynFNC) to evaluate evidence of brain response to TMS. Results show clear functional dynamic patterns categorized by frequency. Some patterns appear to be more directly linked to TMS, but there is one pattern that might be a TMS-independent response to the excitation. This first look presents an analysis methodology and important results to consider in future research.**

I. INTRODUCTION

The brain can be viewed as a collection of functional networks each exhibiting different changes in neuronal activity [1]. An important line of research focuses on characterizing the mechanisms by which these networks interact. One of the most important tools in this field is transcranial magnetic stimulation (TMS) designed to stimulate neuronal tissue through exposure to time varying magnetic fields [2]. This technique allows observing the response of the brain to specific stimulations mainly defined by frequency and location. However, the effects this stimulation has in the brain are poorly understood.

The use of TMS is closely related to assessments of time varying brain activity such as in functional magnetic resonance imaging (fMRI). Several studies have observed brain activity responses to TMS for frequencies between 5 Hz and 20 Hz [3, 4]. One of the preferred areas to stimulate is the dorsolateral prefrontal cortex (dlPFC). A large number of both cortical and subcortical structures have projections to the dlPFC, which is often implicated in "top-down" modulation of cognitive functions [5]. TMS stimulation of dlPFC has been implicated in the study of major depression [6], anxiety [7] and bipolar [8] disorders.

Although TMS has been mainly used for the study of time varying brain activity, more recent trends are studying the responses of functional connectivity to TMS [9]. Most functional connectivity studies focused on task-free resting state experiments. Resting state functional connectivity analyses assess a connectivity value representing the synchronicity strength (e.g. correlation) between time changing activations of two brain areas.

The current work aims at identifying dynamic resting state functional connectivity responses to TMS. For this purpose, we employed a technique known as dynamic functional network connectivity (dynFNC) that tracks patterns of time varying functional connectivity among functionally independent brain networks [10]. In this exploratory analysis, we stimulated an area of the dlPFC during a fMRI scanning and estimated the time variations of dynFNC. We then assess the different dynFNC frequencies excited by the stimulation linking the response to iterations and repetitions of connectivity patterns through time.

II. METHODS

A more detailed description of data collection and analysis can be found in a previous report [11].

A. Subjects

This experiment collected data from six healthy subjects (3 males and 3 females between 24 and 37 years) with no medical and no neurological history of problems including brain injury, loss of consciousness, or psychiatric diseases. All participants signed informed consent. Experimental procedures were ratified by the Georgia Tech Institutional Review Board.

B. Experimental Procedure

Each participant went through two sessions separated by less than one week. Four different conditions were considered with different frequencies of stimulation. Thirty TMS pulses were given for each condition differing by the deposition rate including 5, 8.33, 12.5, and 25 Hz (Figure 1). Each of the four frequencies was chosen based on the acquisition time (40 ms) of a single fMRI slice. Each TMS pulse was arranged to affect only one single fMRI slice. Thus, TMS pulses were delivered every 1, 2, 3, or 5 slices with stimulation frequencies of 25, 12.5, 8.33, and 5 Hz, respectively. In all conditions, TMS intensity was set to 100% of motor threshold with three TMS runs in each session. Each run was organized in 5 blocks of four trials. Conditions were delivered in a randomized order for a total of 1,800 TMS pulses (3 runs x 5 blocks x 4 trials/block x 30 pulses per trial) in each session. The distance between the onsets of consecutive trials was set to 31 seconds or 25 fMRI volumes. Each run thus lasted 682 seconds.
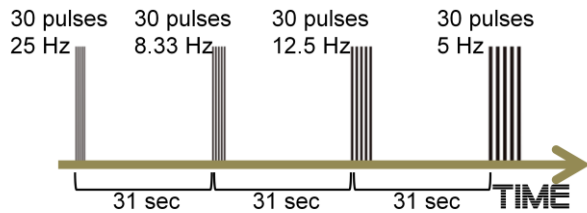
V. M. Vergara and V.D. Calhoun are with the Tri-Institutional Center for Translational Research in Neuroimaging and Data Science (TReNDS), Georgia State University, Georgia Institute of Technology, and Emory University, Atlanta, GA, USA (corresponding author V.M.V.: 1-404-413-4962; e-mail: vvergara@gsu.edu).

F. Rafiei and D. Rahnev are with Center of Advanced Brain Imaging (CABI) and School of Psychology, Georgia Institute of Technology, Atlanta, GA, USA

M. E. Wokke is with The Graduate Center of the City University of New York, New York, NY, USA

H. Lau is with The Brain Research Institute and Department of Psychology, University of California, Los Angeles, CA, USA.

Figure 1. Experimental design. Four interleaved conditions with frequencies 5, 8.33, 12.5, and 25 Hz. Figure shows an estimated stimulation spot.

C. TMS delivery and MRI protocol

The stimulation area was set in left dlPFC (Fox et al., 2012). Based on a previous resting state fMRI experiment, the stimulation spot was defined as the voxel in the left middle frontal gyrus with strongest anti-correlation with the subgenual nucleus.

TMS protocols were within safety limits [12]. Participants did not report any atypical discomfort or symptom either during or after the experiment. TMS equipment consisted of a magnetic stimulator (MagPro R100, MagVenture), using an MRI-compatible figure of eight coil (MRI-B90). The resting motor threshold (RMT) was determined immediately prior to the main experiment. The motor cortex was located by applying supra-threshold single pulses. The final location of the motor cortex was the region that induced maximal contralateral finger twitching on 5 out of 10 trials. The average RMT was 60.67 (SD = 2.42).

Scans were acquired from a Siemens 3T Trio scanner. The TMS coil was too large to fully fit into the MRI receiver coils. For this reason, we employed a setup that consists of the bottom part of a 12-channel MRI coil together with a 4-channel FLEX coil that wraps on the top of the subject. This allowed us to obtain full brain coverage. High resolution T1-weighted anatomical images were acquired with an MPRAGE pulse sequence (FoV = 256 mm; TR = 2250 ms; TE = 3.98 ms; 176 slices; flip angle = 9˚; voxel size = $1.0 \times 1.0 \times 1.0$ mm^3). Functional images were acquired using a T2*-weighted gradient echo-planar imaging sequence using a TR of 1,240 ms and 31 descending slices (40 ms per slice). Other parameters are FoV = 220 mm; TE = 30 ms; flip angle = 50˚; voxel size = $3.0 \times 3.0 \times 3.5$ mm^3.

D. Preprocessing

Data were analyzed using a combination of SPM12 and AFNI. DICOM images were transformed to NIFTI format. All TMS-related artifacts were removed using interpolation. Images were despiked using AFNI's 3dDespike. The following steps were applied: slice-time correction, realignment to the first volume, co-registration to the anatomical image acquired at the beginning of the session (reference image), normalization to MNI space, and spatial smoothing with a 6 mm full width half maximum (FWHM) Gaussian kernel.

Data were subject to a group independent component analysis (gICA) using the GIFT software (https://trendscenter.org/software/gift/) to obtain a set of 70 components. Artifactual components were detected and discarded based on their relationship with white matter, cerebrospinal fluid and frequency.

E. Dynamic Functional Connectivity

Not all ICA components were related to TMS. Relevant TMS components were selected by inspection of their frequency power spectrum. A strong frequency component of 1/31 Hz was used as selection criterion which is based on the TMS delivery lapse of 31 seconds. In addition and similar to other FNC analyses, a final selection of 15 components was decided after excluding any suspicion of movement artifacts, located at cerebrospinal fluid or white matter. The selected 15 components were grouped according to their spatial location into sensorimotor, visual and temporal domains. One exception was a component in the putamen that was assigned to the temporal domain due to its correlation with those components. The filtered sliding window correlation (FSWC) method [13] was used to estimate dynFNC using a finite impulse response filter of 50 taps (50×TR = 62 sec) with a low pass cut-off of 0.05 Hz. Notice that regular sliding window correlation would have a much lower cutoff at 0.016 Hz (1/[62 sec]) thus we achieve higher frequency response with the FSWC method. Derivatives of dynFNC (DdFNC) were estimated using the discrete central difference method [14].

A k-means clustering algorithm with 9 clusters was applied to the concatenation [dynFNC, DdynFNC]. The number of clusters was found using the Ray-Turi method [15]. We analyzed the membership function and the dynFNC data for patterns in the time evolution data.

III. RESULT PATTERNS IN DYNFNC

A. Main frequency components

We plotted the mean power spectral density (PSD) for all dynFNCs in Figure 2a and found several frequencies of importance. The main frequency component of the PSD coincides with the block design cycle of 0.032 Hz (1/31sec). This component is expected given the experimental design.
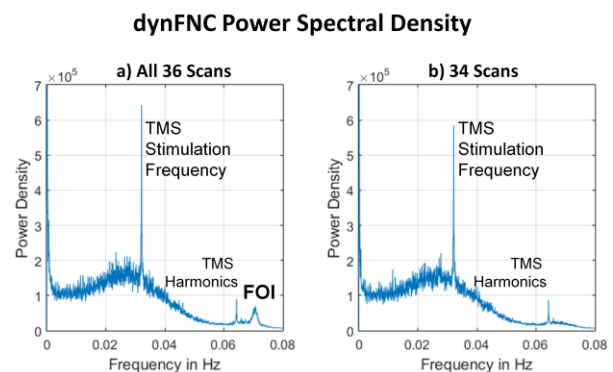

Figure 2. Mean PSD for the dynFNC for selected ICA components. In, a) all subjects where included. In b) two outlier subjects exhibiting a 0.0706 Hz frequency of interest (FOI) were removed.

The second strong PSD component corresponds to the first harmonic 0.064 HZ of the block design repetition. However, there is a component at 0.0706 Hz that did not correspond to the block design and might indicate a natural frequency response. After further analysis, we found that such frequency appears in one of the scans as a very strong oscillation. In addition, there is a brief appearance of that frequency in one other scan. If the outlier scans are removed

the frequency of interest (FOI) 0.0706 Hz does not appear in the PSD as illustrated in Figure 2b.

B. Centroids of dynFNC clusters

We plot the static FNC in Figure 3 for further reference. There are no derivatives for static FNC since this method doesn't consider time variability. Instead, Figure 3 gives us a reference baseline of overall connectivity.
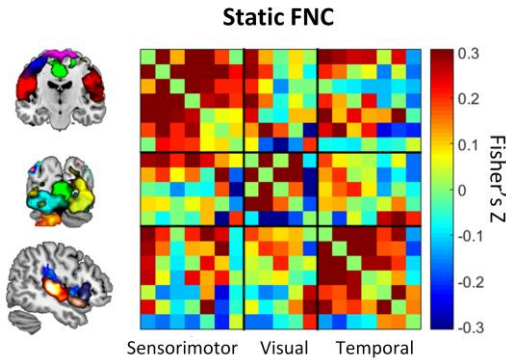

Figure 3. Static FNC from the group ICA.

For dynFNC, the k-means clusters define 9 different connectivity matrices that most closely match the dynFNC at a given point in time according to the membership function. The centroids can be seen in Figure 4. Since we are including derivatives in the analysis, we were expecting to see pairs of similar patterns but opposite derivatives [14]. Out of the 9 clusters only one such pairs were observed between clusters 1 and 2. Figure 4 shows centroids and derivatives matching across all clusters.

C. Tracking dynFNC clusters

In any given scan, each cluster has limited time duration before the dynFNC becomes more similar to the pattern of a different cluster. We were interested in the probability of transitioning from a given cluster X_{prev} to a different one X_{next}. We can express this probability as $P(X_{next}|X_{prev})$ indicating the chance to move to a cluster X_{next} that given the current cluster is X_{prev}.

Figure 5a shows the results and the interpretation of dynFNC. In case the dynFNC happens to be in cluster 1 or 2, an oscillatory behavior will occur indicated by the values of $P(1|2)$ and $P(2|1)$ being close to one (see Figure 5b). This oscillation was strongly observed in one subject and briefly in another one. The most probable transitions involve either cluster 4 to 9 transitioning into cluster 3. We made an alternative analysis and removed the two subjects where clusters 1 and 2 oscillation happened. Coincidentally, these two scans are the same two scans causing the appearance of the FOI of Figure 2. Thus, transitions among clusters 3 through 9 are not related to the 0.07 Hz FOI.

Figure 5b shows the conditional probability matrix which numerically confirms the diagram of Figure 5a. Based on the conditional probabilities it is easy to hypothesize that cluster 3 is the most frequent cluster. Figure 3c illustrates this observation. We calculated the fraction time (FT) or the percentage of time (out of the total scan time) each cluster lasted. FT in cluster 3 was significantly the most visited

cluster, thus confirming the hypothesis. On the other hand, both clusters 1 and 2 were significantly the least visited of all other clusters, but there was no difference between them.
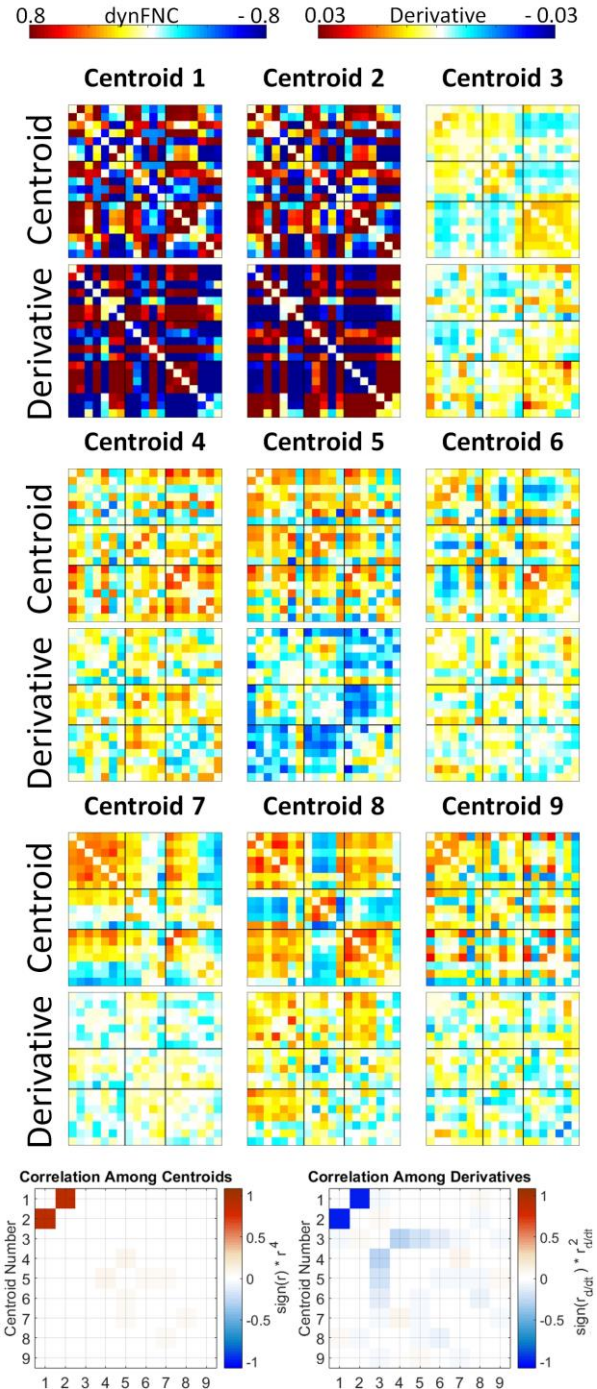

Figure 4. Centroids from kmeans clustering and their similarity matching. Each centroid consists of dynFNC and its derivative DdFNC.

C. Tracking transition frequencies

We first analyzed the 0.07 Hz FOI because a relationship with the experimental block design duration (with frequency of 0.032 Hz) seems unlikely. Notice, 0.07 Hz does not coincide with any harmonic of 0.032 Hz. The frequency 0.07 Hz along with clusters 1 and 2 were only detected in two scan session.
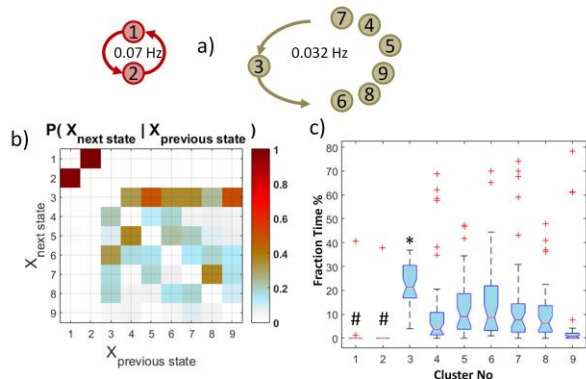
Figure 5. Temporal dynamics of the nine clusters: a) Results interpretation and conceptual diagram; b) Transition probability map; c) Fraction Time in %. *-significantly higher. # - significantly lower.

We created a t-sne plot to visualize the relationship among clusters. Figure 6 shows clusters 1 and 2 manifest as separate from the other clusters. Figure 6 also shows the membership function plot of the scan where the oscillatory behavior was observed. Such oscillations happened for a relatively long period with a frequency of 0.07 Hz. For sanity check, we removed the two scans with the 0.07 Hz to repeated k-means and t-sne resulting in a single t-sne cluster where state 1 and 2 did not exist. It is now straight forward to link functional dynamics of the other clusters (3 to 9) to regular dynFNC. The dynamic behavior can be summarized by moving in and out of cluster 3 into any of the other related clusters.
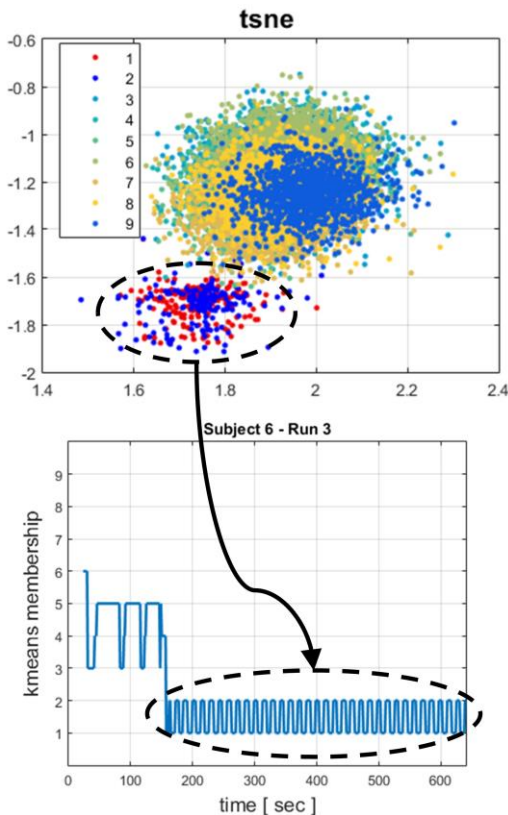

Figure 6. Oscillatory behavior of 0.07 Hz observed in the memberships function and its segregation visualized using t-sne.

IV. DISCUSSION

This exploratory analysis revealed patterns of temporal dynFNC as a response to TMS delivered into the dlPFC. Two frequency patterns were observed. One frequency coincides with the time between stimulations. The other frequency response could not be directly linked to the stimulation period. Clustering dynFNC showed specific connectivity patterns that are easy to separate as demonstrated by the low dimensional embedding algorithm t-sne.

Energy deposition into the dlPFC via TMS results in a propagation of signals activating distant parts of the brain [16] including the motor cortex [17]. We found three frontal lobe components in the ICA decomposition with existing, but weak frequency at 0.032 Hz. This frequency corresponds to the initiation and rest lapse of 31 sec between stimulations, see Figure 1. ICA time courses from sensorimotor, visual and temporal areas had higher power at the 0.032 Hz higher frequency component. Thus, our analysis focused on brain areas with the stronger response assuming that delivered TMS frequencies (>5 Hz) produce excitability. This assumption is based on previous studies confirming the expected excitation. High frequency (>5 Hz) stimulation produces increased, while low frequency (<5 Hz) brings decreased, excitability [18, 19].

The frequency response in Figure 2 clearly shows that dynFNC exhibit the 0.032 Hz frequency and its harmonics, plus an addition component in 0.07 HZ. These frequencies correspond to dynFNC (connectivity between 2 brain networks) and are conceptually different from the brain network activity (time varying activity measured for a single brain network). Our data shows that peak dynFNC frequency coincide with the periodic lapse between stimulations of 31 seconds. The exception is the 0.07 Hz frequency which has no apparent link to the stimulation frequencies or the lapse between stimulations. It is possible that the outlier 0.07 Hz is solely a biological response observable from dynFNC data rather than an artificially stimulated oscillation.

Connectivity associated to the 0.07 Hz exhibit relatively strong correlations and anti-correlations see cluster 1 and 2 in Figure 4. Considering that two out of 36 scans exhibited this frequency, we can conclude that such occurrence is not common and might be related to some unusual brain response. However, we lack the data to confirm this hypothesis.

Observed dynFNC is characterized by a large preference to exhibit the pattern of cluster number 3. This is confirmed by the significantly larger FT of cluster 3 compared any other cluster and the conditional probability $P(X_{next}|X_{prev})$ maps. We can argue that cluster 3 is the common preferred state of any subject, while the other clusters are driven by subject specific variability. Thus, dynamics of TMS response was followed by interplay between induced cluster 3 and less predictive connectivity patterns.

Although the experiment included different TMS frequencies, we did not observe differences in the dynFNC strength. This might be a limitation due to the relative slow TR of 1.24 sec which does not have enough resolution to properly analyze frequencies of 5 Hz or higher.

REFERENCES

[1] E. Bullmore and O. Sporns, "Complex brain networks: graph theoretical analysis of structural and functional systems," *Nat Rev Neurosci,* vol. 10, pp. 186-98, Mar 2009.

[2] M. Hallett, "Transcranial magnetic stimulation: a primer," *Neuron,* vol. 55, pp. 187-99, Jul 19 2007.

[3] A. Pascual-Leone, J. M. Tormos, J. Keenan, F. Tarazona, C. Canete, and M. D. Catala, "Study and modulation of human cortical excitability with transcranial magnetic stimulation," *J Clin Neurophysiol,* vol. 15, pp. 333-43, Jul 1998.

[4] A. M. Speer, T. A. Kimbrell, E. M. Wassermann, J. D. Repella, M. W. Willis, P. Herscovitch*, et al.*, "Opposite effects of high and low frequency rTMS on regional brain activity in depressed patients," *Biological Psychiatry,* vol. 48, pp. 1133-1141, 2000.

[5] E. K. Miller, "The prefrontal cortex and cognitive control," *Nat Rev Neurosci,* vol. 1, pp. 59-65, Oct 2000.

[6] M. Avissar, F. Powell, I. Ilieva, M. Respino, F. M. Gunning, C. Liston*, et al.*, "Functional connectivity of the left DLPFC to striatum predicts treatment response of depression to TMS," *Brain Stimul,* vol. 10, pp. 919-925, Sep - Oct 2017.

[7] M. Balconi and C. Ferrari, "Left DLPFC rTMS stimulation reduced the anxiety bias effect or how to restore the positive memory processing in high-anxiety subjects," *Psychiatry Res,* vol. 209, pp. 554-9, Oct 30 2013.

[8] R. Kazemi, R. Rostami, S. Khomami, G. Baghdadi, M. Rezaei, M. Hata*, et al.*, "Bilateral Transcranial Magnetic Stimulation on DLPFC Changes Resting State Networks and Cognitive Function in Patients With Bipolar Depression," *Front Hum Neurosci,* vol. 12, p. 356, 2018.

[9] L. Beynel, J. P. Powers, and L. G. Appelbaum, "Effects of repetitive transcranial magnetic stimulation on resting-state connectivity: A systematic review," *Neuroimage,* vol. 211, p. 116596, May 1 2020.

[10] E. A. Allen, E. Damaraju, S. M. Plis, E. B. Erhardt, T. Eichele, and V. D. Calhoun, "Tracking whole-brain connectivity dynamics in the resting state," *Cereb Cortex,* vol. 24, pp. 663-76, Mar 2014.

[11] F. Rafiei, M. Safrin, M. E. Wokke, H. Lau, and D. Rahnev, "Transcranial magnetic stimulation alters multivoxel patterns in the absence of overall activity changes," *Hum Brain Mapp,* vol. 42, pp. 3804-3820, Aug 15 2021.

[12] S. Rossi, M. Hallett, P. M. Rossini, A. Pascual-Leone, and T. M. S. C. G. Safety of, "Safety, ethical considerations, and application guidelines for the use of transcranial magnetic stimulation in clinical practice and research," *Clin Neurophysiol,* vol. 120, pp. 2008-2039, Dec 2009.

[13] V. M. Vergara and V. D. Calhoun, "Filtered correlation and allowed frequency spectra in dynamic functional connectivity," *J Neurosci Methods,* vol. 343, p. 108837, Jul 1 2020.

[14] F. Espinoza, E. Damaraju, V. Vergara, K. Henke, J. Turner, and V. Calhoun, "Characterizing whole brain temporal variation of functional connectivity via zero and first order derivatives of sliding window correlations," presented at the Sixth Biennial Conference on Resting State and Brain Connectivity, 2018.

[15] V. M. Vergara, M. Salman, A. Abrol, F. A. Espinoza, and V. D. Calhoun, "Determining the number of states in dynamic functional connectivity using cluster validity indexes," *J Neurosci Methods,* vol. 337, p. 108651, May 1 2020.

[16] J. J. T. Vink, S. Mandija, P. I. Petrov, C. A. T. van den Berg, I. E. C. Sommer, and S. F. W. Neggers, "A novel concurrent TMS-fMRI method to reveal propagation patterns of prefrontal magnetic brain stimulation," *Hum Brain Mapp,* vol. 39, pp. 4580-4592, Nov 2018.

[17] B. Fierro, M. De Tommaso, F. Giglia, G. Giglia, A. Palermo, and F. Brighina, "Repetitive transcranial magnetic stimulation (rTMS) of the dorsolateral prefrontal cortex (DLPFC) during capsaicin-induced pain: modulatory effects on motor cortex excitability," *Exp Brain Res,* vol. 203, pp. 31-8, May 2010.

[18] S. K. Esser, R. Huber, M. Massimini, M. J. Peterson, F. Ferrarelli, and G. Tononi, "A direct demonstration of cortical LTP in humans: a combined TMS/EEG study," *Brain Res Bull,* vol. 69, pp. 86-94, Mar 15 2006.

[19] A. Valero-Cabre, B. R. Payne, and A. Pascual-Leone, "Opposite impact on 14C-2-deoxyglucose brain metabolism following patterns of high and low frequency repetitive transcranial magnetic stimulation in the posterior parietal cortex," *Exp Brain Res,* vol. 176, pp. 603-15, Feb 2007.